

FAST-OAD-GA: AN OPEN-SOURCE EXTENSION FOR OVERALL AIRCRAFT DESIGN OF GENERAL AVIATION AIRCRAFT

Florent Lutz¹, Joël Jézégou¹, Aurélien Reysset², Aitor Busteros Ramos¹ & Valérie Pommier-Budinger¹

¹ISAE-SUPAERO - Université de Toulouse, 31055 Toulouse, France

²INSA Toulouse, 31400 Toulouse, France

Abstract

In order to respond to the growing need for a reduced environmental footprint of the commercial aviation sector, new aircraft architecture and propulsion technology have become a major focus in the aerospace research field. In this context, many new projects featuring innovative configurations or powertrains, for which light aircraft are under consideration as final products or as small scale test platforms for larger airplane, have taken shape. The assessment of the feasibility of such concepts requires an Overall Aircraft Design (OAD) study at a preliminary stage in order to rule out non-viable design choices and identify key features. Consequently, OAD tools play a key role during the conceptual design phase as they allow to automatically carry out said studies and, using their Multidisciplinary Design Analysis and Optimization capabilities, identify the most likely design. FAST-OAD-GA, an open-source extension of FAST-OAD completes the aircraft design techniques from FAST-OAD with general aviation specific models to enable the preliminary sizing of aircraft regulated by the EASA CS-23. This paper presents the FAST-OAD framework, its capabilities, the models added by FAST-OAD-GA for general aviation aircraft sizing and the upcoming changes to model innovative architectures.

Keywords: Overall Aircraft Design, General Aviation, FAST-OAD, MDAO

Nomenclature

AOA	Angle of Attack
CC	Combustion Chamber
CG	Center of Gravity
FAST-OAD	Future Aircraft Sizing Tool - Overall Aircraft Design
FAST-OAD-GA	Future Aircraft Sizing Tool - Overall Aircraft Design - General Aviation
ft	Feet
hp	Horsepower
HPT	High Pressure Turbine
HTP	Horizontal Tail Plane
ICE	Internal Combustion Engine
ITT	Inter Turbine Temperature
kW	Kilowatt
MDAO	Multi-Disciplinary Analysis and Optimization
MEP	Mean Effective Pressure
MTOW	Max Takeoff Weight
nm	Nautical mile
OAD	Overall Aircraft Design
OPR	Overall Pressure Ratio

PIM	Pilot's Information Manual
POH	Pilot's Operating Handbook
PT	Free Power Turbine
SFC	Specific Fuel Consumption
TAS	True Air Speed
TLAR	Top Level Aircraft Requirements
VLM	Vortex Lattice Method
VTP	Vertical Tail Plane

1. General Introduction

Within the context of the reduction of the impact of aviation on the climate, a major research effort has been put into motion towards achieving greener aircraft. Some promising leads have been identified as means to reduce the CO₂ emissions, such as the introduction of electric technologies inside the propulsion chain or optimizing the aero-propulsive interactions [1]. These technologies however come with their own set of opportunities and challenges, each bringing their own different optimal design parameters which are not always compatible. The integration of these technologies must thus be conceptually evaluated at the aircraft level to quantify the consequence on their performance. For instance, the environmental impact of the integration of a fuel-cell based propulsion system on a 80 seat regional airplane is studied in [2]. Likewise, the feasibility of a 10 seat CS-23 all-electric aircraft with a range of 500 nm is explored in [3]. More disruptive concepts have also been investigated at the conceptual level, among which is the use of distributed propulsion. Because of the greater lift coefficient achievable using this effect, aircraft could theoretically have smaller wings, reducing the profile drag [4]. Distributed propulsion could also have a positive impact on the structural weight of the wing [5], but at the cost of a heavier propulsion system. Because of the numerous coupling brought forth by new propulsion technologies and architectures, the multidisciplinary characteristic of the aircraft design is ever more present, highlighting the need for tools and methods capable of handling Multi-Disciplinary Analysis and Optimization (MDAO).

The assessment of the feasibility of such new concept is carried out during the conceptual design phase, in which the viability of the configuration can be checked. During this phase time-efficient methods are used to quickly identify the design trends and rule out unfeasible configurations without going into very detailed studies. However, due to the multi-disciplinary nature of aircraft design and because the process is highly iterative, software were developed to help automating the process. SUAVE is a conceptual level aircraft design environment coded in Python and developed by the University of Stanford which provides user with the ability to work on both conventional and unconventional designs [6]. TASOPT (Transport Aircraft System OPTimization) is a program from MIT and written in Fortran77, which relies on low-order physical method rather than statistical formulas [7], making them more fit for the evaluation of unconventional architectures than traditional statistical methods. More recently, ISAE-SUPAERO and ONERA have started working on an aircraft design software based on the OpenMDAO framework [8] called FAST-OAD [9].

This paper aims at presenting FAST-OAD-GA, an open source extension of the FAST-OAD framework with models specifically tailored for General Aviation aircraft. In the first section, the FAST-OAD framework will be discussed along with its limitations regarding the sizing of CS-23 aircraft. Next, the models used in the current distribution of FAST-OAD-GA will be presented. These models will then be validated against two CS-23 airplane. Finally, the ongoing work on the adaptation of the code for innovative aircraft configurations will be reviewed.

2. The FAST-OAD framework

FAST-OAD is an open-source aircraft sizing and optimization tool developed by ISAE-SUPAERO and ONERA. It is based on the OpenMDAO framework and a previous sizing tool called FAST developed since 2015. To fully use the MDAO capabilities of OpenMDAO, the aircraft sizing methodologies have been written as components. In addition, FAST-OAD uses a variable naming convention which makes

clear what each data refers to and allows for easier interfacing of the methodologies. This makes the handling of the multidisciplinary aspect of aircraft design easier for the end user. Moreover, thanks to the models system put into place, it is easy to add/remove models from the process. This is done with the help of a configuration file which is where the management of the models is centralized. This all makes the FAST-OAD framework a very flexible tool for aircraft design and opens the way for the integration of custom models and the revision of existing ones to accommodate for the analysis of new aircraft configurations.

FAST-OAD codes come by default with models adapted for CS-25 aircraft which are grouped by aircraft design disciplines. It includes: Geometry, Aerodynamics, Weight and Performances among others. Those disciplines and the way they are connected in a typical FAST-OAD run are illustrated in Figure 1.

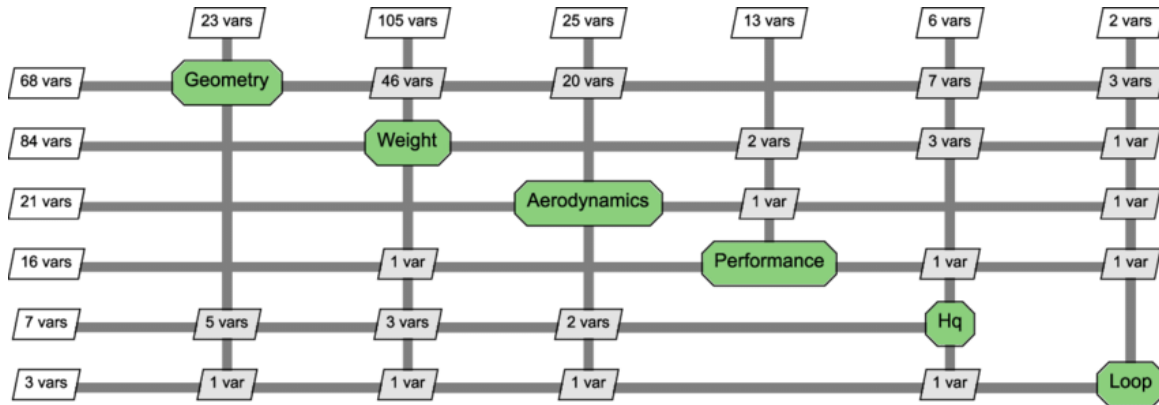


Figure 1 – FAST-OAD disciplines interrelationship [9]

Even though the FAST-OAD framework has been extended for the preliminary sizing of unconventional architectures with the works described in [10] and [2], which proves the adaptability of the framework, the models used in the current open-source distribution correspond to a classical tube and wing configuration. Said models are valid for commercial transport aircraft and the code uses an A320-type aircraft as reference. The detailed mass breakdown of the empty aircraft is obtained using a collection of empirical correlations taken from [11] and [12], whose domain of validity is limited to commercial transport aviation. The loads on the basis of which these weights are computed are determined according to the requirement imposed by the FAR25. Finally, the propulsion of the aircraft is a rubber engine whose model is extracted from [13]. It is based on a reference turbofan engine and can be scaled according to various design parameters.

For the design of general aviation aircraft using FAST-OAD, two limitations have to be considered. First, the statistical formulas such as the ones used in the open-source distribution of FAST-OAD tend to lose accuracy when used on aircraft bearing lots of differences with the one used to establish the equations. Secondly, very few certified CS-23 aircraft are equipped with turbofan/turbojet engines. Therefore, general aviation aircraft were out of the scope of the aircraft being able to be modeled with the tool as it was. The sizing loops however remain the same for any fuel burning aircraft with conventional architecture and are thus inherited from FAST-OAD. This leads to the implementation of new models, specific to light aircraft, bundled as an extension of FAST-OAD, hence keeping its MDAO capabilities, and named FAST-OAD-GA.

3. Models in FAST-OAD-GA

This section is dedicated to the presentation of the models that have been changed from FAST-OAD [14] for the release of the open-source version of FAST-OAD-GA.

3.1 Aerodynamics

For the computation of the drag polar of the aircraft, a simple parabolic model to which the trim drag is added as presented in Equation 1 is used.

$$C_D = C_{D0} + k_{wing} * C_{l,wing}^2 + C_{D,trim} \quad (1)$$

By default when launching a FAST-OAD-GA run, a Python implementation of a VLM code is used. It enables to compute the 3D lift curve of the wing and, by accounting for the downwash at the tail, the lift curve of the Horizontal Tail Plane (HTP). It also provides an estimation of the induced drag coefficient used in Equation 1. The parasitic drag is computed using the component drag buildup method presented in [15]. Finally, the trim drag is computed by taking into account the drag induced by the lift the HTP has to produce to balance the aircraft as well as the profile drag caused by the use of the elevators. This is illustrated by Equation 2.

$$C_{D,trim} = k_{htp} * C_{l,htp}^2 + C_{D,\delta_m} * \delta_m \quad (2)$$

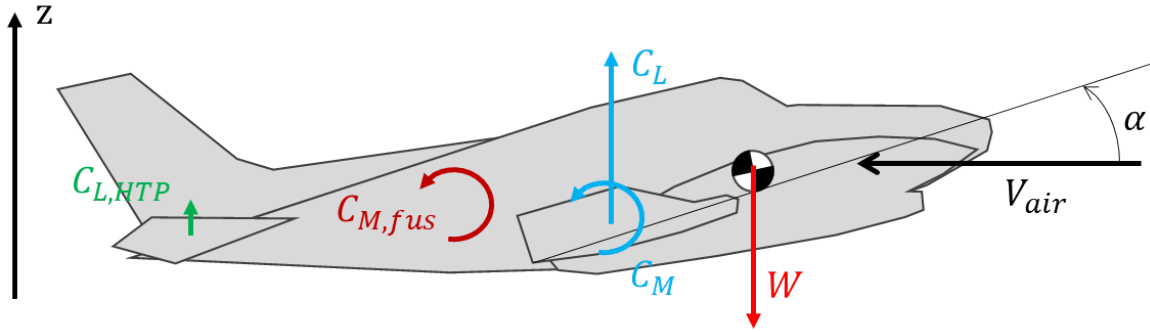


Figure 2 – Forces considered in the lift equilibrium of the aircraft

The aircraft equilibrium (Figure 2) consists in solving a system of two equations (vertical and rotational dynamics) with two unknowns: wing lift $C_{l,wing}$ and HTP lift $C_{l,htp}$ for a given vertical acceleration \ddot{z} , dynamic pressure q , aircraft geometry and weight W (aircraft weight and gravity center can evolve with time). Making the assumption of small angle ϕ (and angle rate $\dot{\phi}$), this leads to the following system of equations:

$$\begin{cases} m * (g + \ddot{z}) = (C_{l,wing} + C_{l,htp}) * q * S_{wing} \\ 0 = [(C_{m,fus} + C_{m,wing}) * l_{0,wing} + C_{l,wing} * (x_{wing} - x_{CG}) + C_{l,htp} * (x_{htp} - x_{CG})] * q * S_{wing} \end{cases} \quad (3)$$

The HTP profile moment is negligible compared to the one induced by its own lift. The wing profile moment is considered constant whatever the Angle Of Attack (AOA) but the one induced by wing lift will vary. As for the fuselage moment term, it is directly proportional to the angle of attack and can be re-written as:

$$C_{m,fus} = C_{m\alpha,fus} * \alpha = C_{m\alpha,fus} * \frac{(C_{l,wing} - C_{l0,wing})}{C_{l\alpha,wing}} \quad (4)$$

This allows to rewrite the system of equilibrium equations 3 to only have $C_{l,wing}$ and $C_{l,htp}$ as unknowns. The calculation process is then quite straightforward. It consists of determining the two lift coefficients from a 2-D acceleration vector. Then the air AOA can be obtained from the wing lift coefficient which allows to compute the lift generated by the HTP itself and the lift generated by the elevator. The drag is subsequently evaluated and thrust is defined to be equal to it. Engine distance to the Center of Gravity (CG) is neglected i.e. thrust does not generate a moment, and its impact on wing/HTP aerodynamics is neglected for now.

This leads to the calculation of equilibrated polars that can be visualized using the basic post-processing tools from FAST-OAD-GA as illustrated in Figure 3.

The VLM code is also used to obtain the distribution of the lift on the wing, which, in conjunction with some automated XFOIL runs on the airfoil selected for the sizing process, enables to estimate the maximum lift coefficient of the aircraft. This lift distribution is also used for the computation of the loads on the aircraft wing.

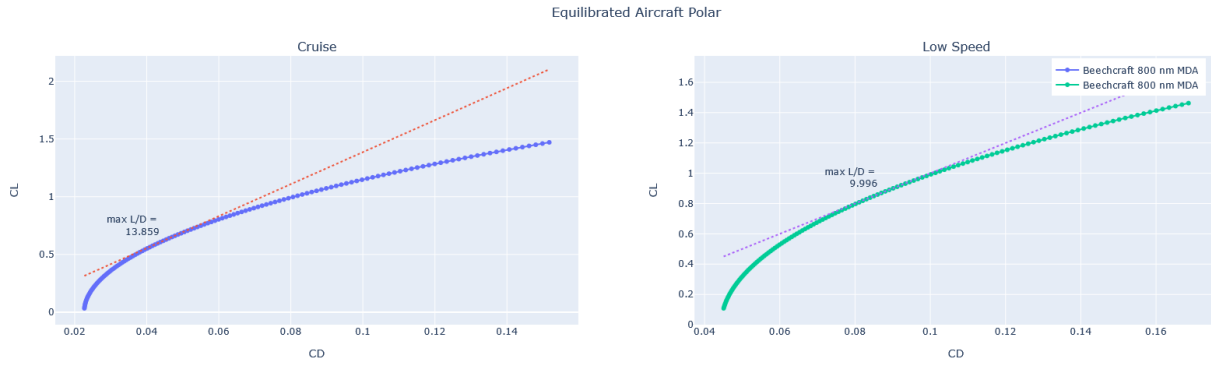


Figure 3 – Equilibrated polar obtained thanks to the post-processing tools of FAST-OAD-GA

The effect of high lift devices and control surfaces is also modeled, using formulas taken from [16], which enables to quantify the behavior of the aircraft in low-speed conditions and simulate a takeoff phase.

Finally, an interface with OpenVSP, an open-source software released under NASA Open Source Agreement as a parametric geometry tool presented in [17], was also implemented. It can be used as a substitute for the VLM method mentioned there above and provides a preliminary estimation of the aircraft aerodynamics using either a vortex lattice or a panel method. It also provides a way to compute the wing-propeller interaction due to the induced velocity using a simple disk actuator model, which can then be used to refine the assessment of the aerodynamic loads on the wing.

The introduction of those slipstream effects in the computation of the performances of the aircraft however entails that the equilibrium method presented before will have to be refined. Indeed, because of the high non-linear coupling between the aerodynamic coefficients and the thrust T , the propulsion equation will not be decoupled from the lift and pitching moment equations anymore. Consequently a solver will need to be used to solve the following 3 equations - 3 unknowns (α, δ_m, T) system:

$$\begin{cases} m * (g + \ddot{z}) = f(q, \alpha, \delta_m, T) \\ m * \ddot{x} = g(q, \alpha, \delta_m, T) \\ 0 = h(q, \alpha, \delta_m, T) \end{cases} . \quad (5)$$

This point will be further discussed in section 5.1

3.2 Geometry

In addition to the wing sizing methodology based on low speed equilibrium and geometrical constraints inherited from FAST-OAD, FAST-OAD-GA provides more detailed methodologies for the sizing of the horizontal and vertical tailplanes.

For the sizing of the HTP, the method presented in [18] has been implemented. It is derived from the computation of the aerodynamic loads on the tail so that it ensures a sufficient angular velocity is achievable during takeoff and landing flareout. It takes into account the CG location of the aircraft and the aerodynamic properties of the wing and the tail.

Similarly to what is done in FAST-OAD, the Vertical Tail Plane (VTP) is sized so that the yaw-moment derivative at aircraft level suggested in [19] can be reached. When applicable (typically in the case of a multi-engine aircraft), sizing cases derived from the certification specifications are also considered to make sure that the aircraft can maintain a straight flight path in case of engine failure during climb and takeoff. Finally, the crosswind landing capabilities of the aircraft are studied following the recommendation of [15] on the sideslip angle and using the methodology presented in [20].

In every case, the sizing margins to the constraints are computed, meaning that it is possible to identify, once the process is converged, which constraints are the most demanding. It also entails that if the areas were to be inputted by the user, it would be possible to ensure that the sizing is correct by asserting that the constraints are respected.

3.3 Load factor

As it is the case in FAST-OAD, some of the mass models bundled in the open-source release rely on the maximum load factor that the aircraft will be subjected to. These load factors can be selected by the aircraft manufacturers but they must comply with the requirements imposed by EASA CS-23. To this end, FAST-OAD-GA provides a method for estimating these load factors which uses the amendment 4 [21] of the CS-23 as an acceptable mean of compliance for the currently applicable performance based amendment 5. This method is based on the search for the maximum load factor inside the flight envelope calculated by FAST-OAD-GA. This envelope is a result of the combination of the maneuver envelope and the gust envelope, which are calculated based on two characteristic masses of the aircraft: the MTOW and the mass of the aircraft with minimum fuel in the wing. An example of flight envelope that can be computed by FAST-OAD-GA is shown in Figure 4.

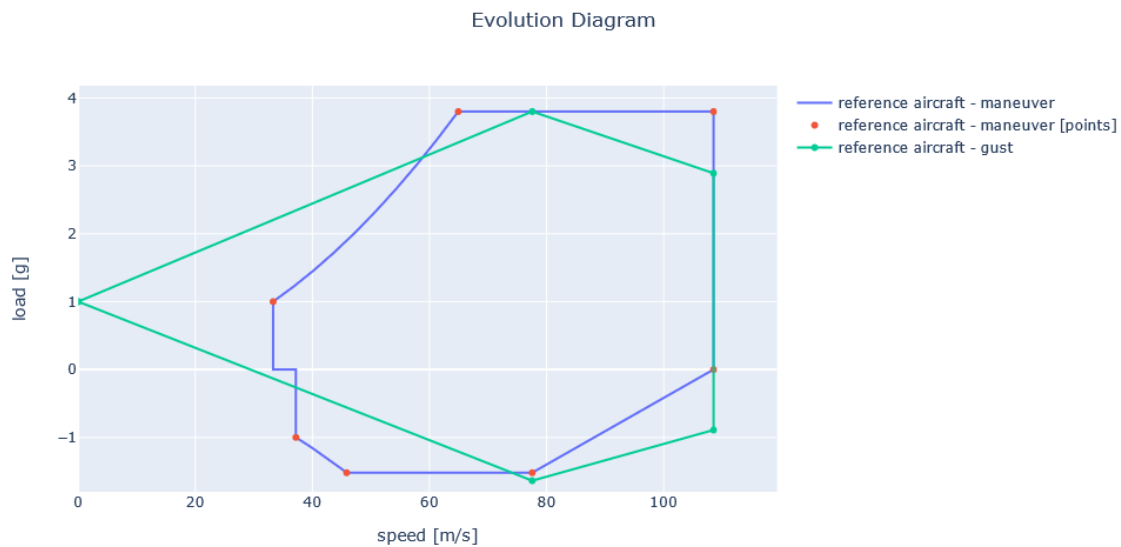


Figure 4 – Evolution diagram obtained thanks to the post-processing tools of FAST-OAD-GA

3.4 Weight

The MTOW of the aircraft is computed by summing the weight of the empty aircraft, the weight of the payload and the weight of the fuel or the alternative energy source that was selected to power the aircraft.

The weight of the payload is simply estimated by the number of passengers and allowed luggage weight on the design mission, which both are user inputs of the code.

The weight of the energy source is computed based on the energy required by the aircraft on a design mission. This mission is defined by the user based on a set of TLARs (*e.g.* range, payload, cruise speed) and a set of performance target (*e.g.* climb rates, descent rate, reserve time). The energy is then computed using a time step integration approach which then enables the mass-performance loop.

For the computation of the empty weight, similarly to what is done in FAST-OAD, the aircraft basic components are separated into several groups, mainly the airframe, the power train, the systems and the furnitures. The basic components weights are then estimated, mostly using semi-empirical formulas taken from [15], [19], [22], [23] and [24]. These however were identified as shortcomings as part of the adaptation of FAST-OAD-GA for the modeling of distributed propulsion aircraft. Indeed, as mentioned above, the presence of distributed propulsion on the wing tends to relieve some of the internal loads on the wing [5] [25], which in turns leads to a lighter wing. This is however not accounted for in the formulas currently used as those were established based on an aircraft with conventional architecture.

To address the limitations of the above-mentioned parametric models, alternative physics based models are being implemented in FAST-OAD-GA. The wing mass for instance can be computed using a method that assess the structural weight necessary to withstand the wing internal loads [26]. It is based on a methodology developed in [27] which was adapted, for the purpose of its integration in FAST-OAD-GA, to take into account the certification specifications from EASA CS-23 [21] as well as the aerodynamic and structural loads stemming from the presence of distributed propulsion on the wing. An example of the forces considered for the structural sizing of the aircraft wing is shown in Figure 5. This method provides coherent results for various aircraft covered by CS-23 and for an unconventional design. The computation of the weight of the fuselage can also be conducted with a physics-based method. This method is adapted from [7] and includes elements from the weight penalty method for fuselage structural weight computation from [18]. First, the fuselage skin thickness is sized to resist pressurization loads or, when not pressurized, based on manufacturing constraints on metal sheet minimum thickness. Then, the weight of additional structural components such as openings, stringers and floor is computed using semi-empirical formula. Finally skin thickness is locally increased to withstand the loads on the fuselage among which are the tail aerodynamic loads and engine loads when applicable.

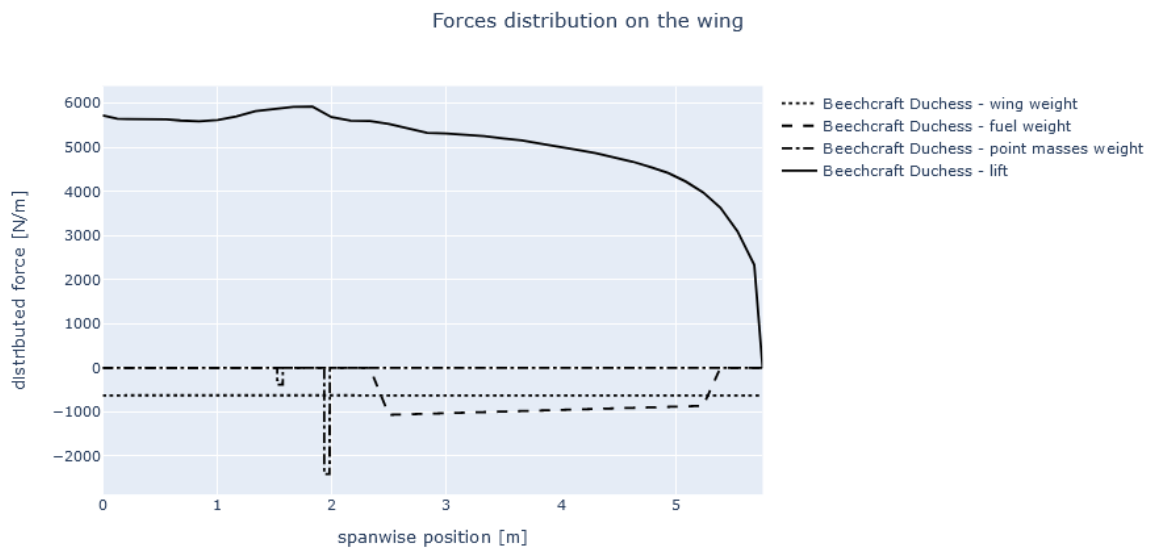


Figure 5 – Example of loads considered in FAST-OAD-GA for the structural sizing of the wing

3.5 Propulsion

A major part of general aviation aircraft are powered by an Internal Combustion Engine (ICE) coupled to a propeller which is the model that was initially implemented. The structure of the code is however already built to accept any type of fuel-based propulsion. As turboprops also represent a significant part of the engines used in CS-23 aircraft, a method was devised to assess the consumption of such engine and was subsequently implemented.

3.5.1 Propeller model

The propeller performances have been modeled with a Blade Element Momentum Theory code coupled with formula from the Actuator Disk Theory. This enables the user to compute the efficiency of the propeller in various flight conditions based on the geometric description provided. This methodology also takes into account the losses at the tip using Prandtl tip loss factor. The results obtained using this process have been compared against two NACA reports [28] [29] and against an open-source propeller design and analysis software called JBLADE. The calculation showed good agreement in the region of highest efficiency but some issues were identified for lowest advance ratio. These inaccuracies are due to the fact that, at low advance ratio, the angle of attack on some part of the blade

is very high making the linearized potential equations no longer valid. This was however not deemed problematic as the propeller efficiency is mostly important for the computation of the energy required for the flight which happens in high speed conditions.

Because of the way this method was implemented, the use of nested solvers was required. In order to minimize the computation time, mainly in the case of a MDAO, an efficiency map of the propeller is produced at the beginning of each run. This way, when doing the computation of the aircraft performance, the only thing left to do is to read the map and interpolate between the points. An example of such a map, obtained for a propeller close to the one of a Beechcraft 76 is shown in Figure 6. This method alone however, does not take into account the installation effects of the propeller which can nonetheless have significant impact on the performances when it is placed in front of a fuselage or nacelle. The main impacts are a reduced efficiency and a shift of the optimal advance ratio due to blockage effects [30]. Consequently, simple models were implemented based on in-house knowledge of the aircraft design team to take those effects into account. The swirl recovery effect of wing on the propeller [31], though it has been identified, has not been treated yet and can thus be considered as a limitation of the model.

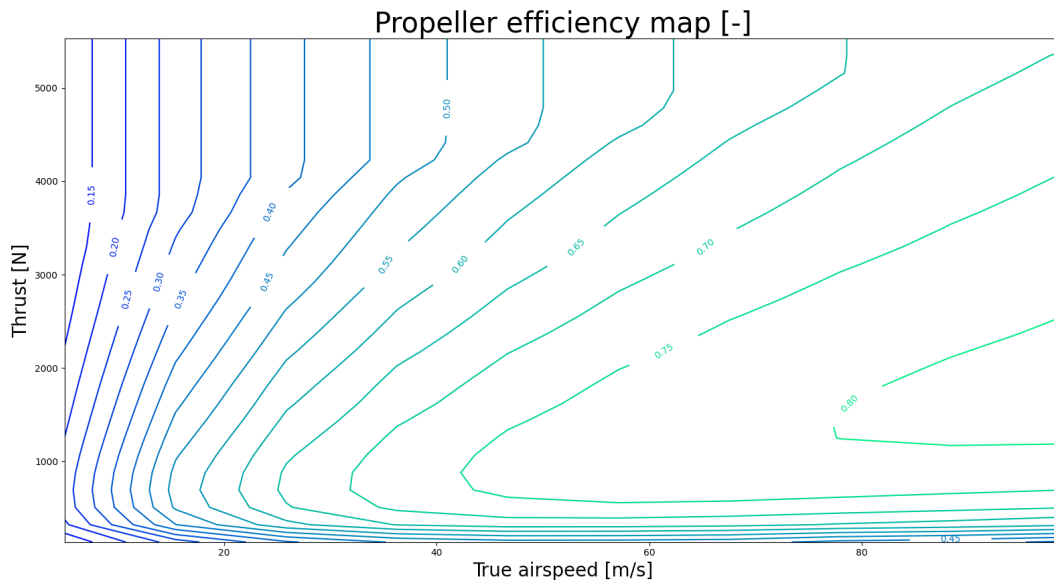


Figure 6 – Propeller efficiency map as computed by FAST-OAD

Once the propeller efficiency is obtained based on the thrust required and flight speed, the shaft power can be computed. Since the ultimate goal is to compute the fuel consumed at each point of the flight in order to perform the time step integration, the fuel consumption of the selected ICE or turboprop in the various flight conditions must be evaluated. This brought forth the challenge of creating models generic enough to be capable of modeling different propulsion systems spanning on a wide range of power.

3.5.2 Internal combustion engine model

ICE modeling was solved by assuming that the fuel consumption of every engine could be obtained by scaling a reference consumption map based on the engine displacement volume assuming a constant maximum Mean Effective Pressure (MEP). This hypothesis of a constant maximum MEP across engines has been verified on a wide range of thermal motors used for aeronautical application for which the values always remained in the range of 19.5 to 19.9 bar. This then enables the computation of the displacement volume of any engine by only knowing its rated power at the specified regime. As for the scale-up of the ICE, it will only hold true for engines from the same technology and architecture as the one selected as the reference. In the case of FAST-OAD-GA, the chosen architecture was a naturally aspirated aeronautical ICE, with 4 or 6 cylinders, which is the most common in CS-23 piston

aircraft. Ultimately, the value of the engine volume allows to compute the MEP that corresponds to each power regime of the new engine. As the $SFC = f(MEP, rpm)$ is assumed to be constant for engines with similar technologies, the computations of the fuel flow for all power regimes for any given engine becomes possible. Consequently, if the Specific Fuel Consumption (SFC) curves can be obtained for a given reference engine, then it will be possible to scale the predictions for any engine of a similar architecture. The engine that was chosen as a reference for this model is the Lycoming O-360 A, which is an atmospheric flat 4-cylinder engine rated at 180 hp, and is a very common engine for light aircraft.

This model was then tested against the fuel consumption data extracted from the Pilot Operating Handbook of the Cirrus SR22 [32] mounting a Continental IO-550-N engine rated at 310 hp, a significantly greater power than the reference Lycoming O-360 A. The results showed good agreement between the actual fuel consumption and the fuel consumption computed based on the scaled results as shown in Table 2.

Table 2 – Fuel consumption comparison between a 310 hp engine obtained with FAST-OAD-GA model and the POH of the Cirrus SR22 at 8000 ft

Engine RPM	Operating Conditions MAP [inHg]	Estimated value [gal/h]	Actual Value [gal/h]	Relative Error [%]
2700	21.7	17.8	18.6	4.3
2600	21.7	17.1	17.8	3.9
2500	21.7	16.8	16.8	0.0
2500	20.7	15.6	15.8	1.2
2500	19.7	14.6	14.8	1.3
2500	18.7	13.7	13.8	0.7
2500	17.7	12.8	12.8	0.0

3.5.3 Turboprop model

For the modeling of the turboprop engine, a different approach was followed. Using thermodynamic equations, the basic geometrical features of a given turboprop are computed by taking into account the known performances of said engine at a given flight point. This point is hereinafter called design point. Once the geometric characteristics of the turboprop are obtained, the performances at any flight point are computed using a simplified representation of the turboprop and the simplifying assumptions presented below. This method can provide physically relevant results adequate for the preliminary design of the aircraft without requiring time-consuming CFD numerical solvers [33].

The following hypothesis were made to model the turboprop engine:

- The engine consists of a single shaft gas generator and a free power turbine that delivers power to the propeller. The gas generator consists of an axial and a radial compressor, a combustion chamber and a pressure turbine.
- The engine is divided into different stations that represent the positions before and after each one of the components where the thermodynamic properties of the air will be computed. As presented in Figure 7, station 0 is the free-stream, station 2 the axial compressor intake, station 25 the stage between compressors, station 3 the end of the compression process, station 4 the exit of the Combustion Chamber (CC), station 41 the entry of the High Pressure Turbine (HPT), station 45 the entry of the free Power Turbine (PT), station 5 the exit of the PT and station 8 the engine exhaust.
- Two bleed offtakes have been modeled : one to account for pressurization and environmental control of the cabin and one for the cooling of the HPT which have been modeled as a mass flow loss after compression. The fuel is added to the air mass flow in station 4 and the cooling bleed air is considered mixed with the burnt gasses in station 41. Mechanical power for aircraft needs is extracted from the HPT [34] and the remaining power is used for the actuation of the propeller

assuming losses in the gearbox and on the shaft. These mass flows and power losses can be either expressed as a constant percentage of the total mass flow or power at the station (such as for power losses) or as a constant absolute value (such as cabin bleed air which depends on the aircraft properties only).

- Between two stations a thermodynamic process takes place: compression, expansion or combustion. Diffusers and the CC are subjected to total pressure losses [33] while turbines and compressors are modeled with polytropic efficiencies [35]. All these parameters can either be chosen by the user from typical literature values or be the reference values provided in FAST-OAD-GA.
- The airflow sections through the HPT and the PT are assumed to always be choked, that is, the local Mach number equals 1. This hypothesis is only true for power regimes over the 40% of the maximum power [36]. As a result of being choked, the relationship between the total temperatures before and after the HPT is constant [35], meaning $T_{45t} = T_{41t} \cdot \alpha$, even in off-design (the name of the constant α is inherited from [33] and [36], it is not to be confused with the AOA). On the other hand, the exhaust section is assumed to be adapted to ambient pressure, a common hypothesis for most turboprops [36].
- A real gas model is used, where C_p and C_v depend on the total temperature of each station [37].

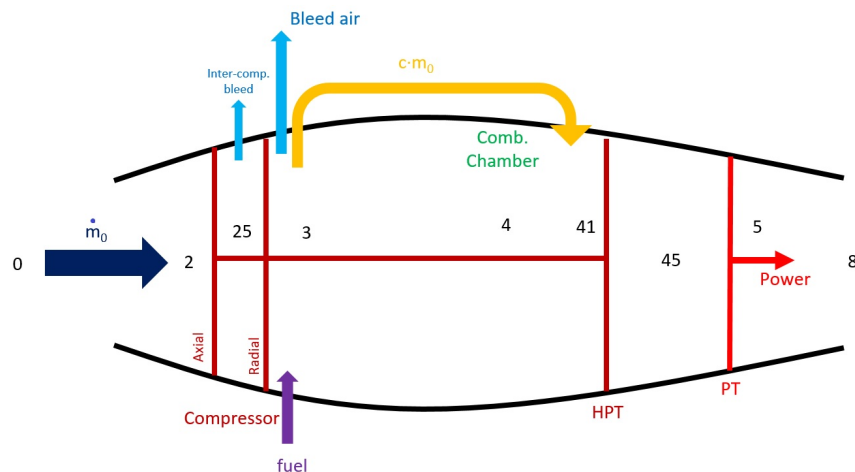


Figure 7 – Scheme of the different stations and components of the turboprop

These assumptions allow to build up a robust model for the computation of the performances of any given turboprop in two steps [33]. Firstly, the geometry of the turboprop must be obtained by recreating the performances at the design point. Because of the hypothesis mentioned above, only 4 fundamental design variables need to be inputted to fully determine the turboprop. The Overall Pressure Ratio (OPR), the equivalent thermodynamic power of the PT, the exhaust Mach (M_8) and the Inter Turbine Temperature (ITT, T_{45t}). In practice, this last value can be replaced by either the SFC or the T_{41t} of the design point, although typically, engine manuals or type certificate data sheets refer only to the ITT.

With these 4 design variables (Power, OPR, ITT and M_8) as inputs (along with all the efficiencies that are assumed to remain constant for all the regimes, as settings) the geometrical parameters can be computed: the sections of the HPT, PT and exhaust (A_{41} , A_{45} and A_8 respectively) as well as the α parameter. These geometrical values remain constant throughout the whole operation [33] [35] [36] and allow to determine the flow circulating through the core for each fuel flow [33] and the thermodynamic parameters at each station. In other words, shaft power is just function of these 4 geometrical values and of the fuel flow, for all flight conditions. This was the main objective of the model: provide an accurate computation of the rated power for a given fuel flow in a turboprop engine. All in all, this means that the 4 design variables at a specific flight point (the design point) fix the 2 turbines and exhaust sections as well as the α parameter which ultimately allow to the computation

of the engine performances at any flight point. Furthermore, the developed model allows to fix the operational envelope of the turboprop engine, which is driven by 3 main constraints: the maximum rated power, the maximum ITT and the maximum OPR. These three restrictions determine in which areas the engine is capable of providing the maximum rated power and in which regions power has to be reduced (by decreasing the fuel flow) to avoid crossing operational constraints.

The developed turboprop model has however some limitations due primarily to some of the hypothesis made. The main drawback is the rigidity of the code to a change of the turboprop architecture, this is, to add or reduce the number of shafts or of any component. This would imply a change in the number of state variables and thus possibly increase the amount of data needed to compute each point of the flight. Secondly, the computations performed for low power regimes (below 40% of the maximum power) will be inaccurate, as α is no longer constant for such power settings [36] due to the PT not being choked in those conditions [33]. These inaccuracies were however deemed acceptable on the OAD level as, under reasonable aircraft parameters, they would only be found during descent which only account for a very small part of the fuel consumed during the mission. Another limitation is that the compressor polytropic efficiency always remains constant due to the lack of accurate compressor maps. This could be solved by adding a routine that adjust generic compressor maps to the required design such as what is done in turboprop simulation software. Finally, transitory states are neglected as well as complex fluid mechanics phenomenons such as turbulent air-fuel mixing phenomena or rotatory effects.

The validation of the model was done using the values offered by the Pilot Information Manual (PIM) of the TBM-700 [34]. Among the different data provided, a set of established altitudes and flight speeds is given with their corresponding fuel flows at maximum power (the achievable maximum power is also specified). Moreover, in this manual it is stated that the maximum ITT is limited to 1070 K, constraint taken into account by the actual model developed.

To replicate the turboprop mounted in the TBM-700, some typical values for component efficiencies have been taken from literature [33][33][37][35]. A study of the engine operational limitations shows that the ITT limit set as input is reached around 25000 for the replicated engine. This can be seen as the power is no longer equal to the gearbox limitation which entails a reduction in the fuel consumed to keep the constraint satisfied. With all these elements taken into account, Table 3, which sums up the performances of the replicated engine, can be computed. Every 5000 ft the maximum power available and fuel flow are computed at the flight speed specified by the manual. Finally, the computed fuel flow and power values are compared against the PIM values.

h (ft)	TAS (KTAS)	P (hp)	P _{PIM} (hp)	Diff. (%)	\dot{m}_{fuel} (kg/h)	$\dot{m}_{fuel,PIM}$ (kg/h)	Diff. (%)
0	230	700	700	0	233	245	-4.8
5000	241	700	700	0	217	221	-1.8
10000	253	700	700	0	202	201	0.5
15000	267	700	700	0	190	186	2.1
20000	281	700	700	0	179	175	2.1
25000	298	691	700	-1	170	169	1.4
30000	298	602	595	1.1	144	142	1.4

Table 3 – Results obtained for the maximum power regime and fuel flow of the PT6A-64 engine (TBM-700).

Overall, the results obtained are fairly accurate with respect to the values offered by the PIM. The computed fuel flows have an error below 5% and below 2% above the 10.000 ft threshold, meaning it can be used for the integration inside a preliminary design tool with satisfactory accuracy.

It should be pointed out that this turboprop module can be used in two different ways. On the one hand it is capable of replicating an existing engine (which implies an accurate knowledge of the performance of its components) as it has been done to validate the results presented in this paper. On the other hand, the model is generic enough to design and obtain the performances of any kind of turboprop engine, even if it is considerably different to the presented one. This is due to the fact that the engine performances are computed using thermodynamic equations that represent the pro-

cesses that take place in each one of its components. Consequently, it is capable of reproducing the performance of general aviation turboprops and of large turboprops with higher rated powers. Nevertheless, it is the responsibility of the user to introduce realistic component performances (efficiencies, air and power losses) if realistic outputs are desired. All things considered, the developed tool provides an accurate simulation of turboprop engines for OAD purposes.

A generic remark that must be made for all the propulsion models is that the values inputted for the engine in the OAD process are fixed and not sized by the process. This means that user knowledge can be required in order to input values that are physically relevant for the aircraft that needs to be assessed. This also means that the design parameter inputted can lead to unfeasible missions that require thrusts above what can be delivered by the system. Checks can however be conducted afterwards on the mission file which monitors the aircraft performance parameters computed at different points of the flight. A check is also carried out at the end of the takeoff computation to ensure that a climb gradient greater than what is imposed by certifications specifications can be reached. This entails that overly small values can quickly be ruled out.

4. Reference aircraft

The viability of the models presented above are assessed through the evaluation of the results of a FAST-OAD-GA run on two of the reference aircraft that are by default bundled with the code. These aircraft are the Beechcraft 76, a typical GA aircraft powered by two ICE, and the Daher TBM 900, a single turboprop high performance aircraft.

The complete list of the inputs necessary for the sizing of those aircraft and their values being available on the FAST-OAD-GA repository [38], only the most relevant ones will be presented below.

4.1 Beechcraft Duchess 76

The Beechcraft 76 is a four-seat twin engine light aircraft. It features a low wing with a T-tail. It is equipped with retractable landing gear and is powered by two Lycoming O-360 engines coupled with two-bladed propellers on the original design [39]. The data that have been used as inputs of the FAST-OAD-GA are either extracted from [39] or they are taken from the Beechcraft 76's POH [40]. It is always assumed that there are two persons in the front pilot seats which explains why in Table 4, the number of passengers is equal to 2 even if it is a four seater.

Table 4 – Main input parameters for the Beechcraft Duchess 76.

Parameter	Value
Number of passengers	2.0
Design range (nm)	711
Design mission speed (KTAS)	158
Design mission altitude (ft)	10000
Approach speed (KTAS)	78
Wing aspect ratio	7.981
Wing airfoil	NACA 63A415
Number of engine	2
Engine rated power (kW)	130

These lead to the main outputs of the FAST-OAD-GA run summarized in Table 5, the full list being available on the FAST-OAD-GA repository [38]. The difference between the outputs of the code and the reference value are less than 6% with the largest difference being on the fuel consumed during the design mission. Further investigation on the fuel consumption in cruise reveals that the engine is not at max power -albeit almost- as opposed to what is shown in the POH, which could explain the difference of fuel consumption. It should be mentioned that the value called MTOW in FAST-OAD-GA includes the fuel consumed during taxi, hence why the reference value in the table, with which the MTOW is compared to, corresponds to the Maximum Ramp Weight. As for the geometrical parameters, the error on the wing area is relatively minor. The active constraint in this case is the

equilibrium at low speed meaning the difference is caused by a slight over-estimation of the maximum lift coefficient. As for the tailplane areas, the fact that both are slightly over the reference data seems to indicate that the computed CG is further aft of the reference one. This is confirmed by the computation of the difference between the output data and the reference one which amounts to 3% of the wing mean aerodynamic chord.

Table 5 – Main outputs for the Beechcraft Duchess 76 run.

Parameter	Output value	Reference value	Diff. (%)
MTOW (kg)	1743	1776	1.9
OWE (kg)	1114	1109	0.2
Fuel mission (kg)	256	272	5.8
Wing area (m ²)	16.66	16.81	0.9
HTP area (m ²)	3.74	3.66	2.2
VTP area (m ²)	1.72	1.70	1.2
Aircraft length (m)	9.23	8.86	4.2

4.2 TBM 900

The TBM 900 is a high-performance single engine turboprop business aircraft with a low-wing and conventional tail configuration. It is powered by a PT6A-66D turboprop engine couple to a five-bladed propeller which allows it to reach cruising speed of up to 330 kts, making it a good representative of the high-performance part of the CS-23. Most of the information for the sizing of the TBM 900 have been taken from the POH [41], from [42] or from promotional material available online [43]. The main inputs are summarized in Table 6. It should be noted that although the wing airfoils on the TBM 900 wing are the RA 16-43 at the root and RA 13.3-43 at the tip, the airfoil used will be the NACA 63A415 because of the lack of data on the formers.

Table 6 – Main input parameters for the Daher TBM 900.

Parameter	Value
Number of passengers	4.0
Design range (nm)	1100
Design mission speed (KTAS)	320
Design mission altitude (ft)	28000
Approach speed (KTAS)	85
Wing aspect ratio	8.22
Wing airfoil	NACA 63A415
Number of engine	1
Engine rated power (kW)	634

As for the Beechcraft 76, the full list of output is available in the FAST-OAD-GA repository [38], but a summary of the results is presented in 7. Because of the specificity of the TBM 900 some of the statistical models used for the computation of the empty weight of the aircraft had to be changed because they were outside the domain of validity. The changes came from the estimation of the weight of the systems and passenger accommodation which are considerably heavier on a high performance aircraft like the TBM 900. Thanks to the submodel feature implemented in FAST-OAD, this was made easy and transparent for the user. This lead to a very good agreement on the estimation of the weight of the airplane with a maximum error of less that 2% for the fuel consumed during the design mission. The turboprop model shows really good agreement on the fuel consumption in cruise with an average of 188 kg/h against 190 kg/h in the PIM [41]. Nonetheless, the computation of the ratio between required thrust for flight and maximum thrust is slightly above 1.0 at the beginning of the cruise phase. This indicates that the computed turboprop is close to its limits which seems coherent with the choice of the cruise speed which is close to the maximum cruise speed that can be reached at that altitude.

For the results on the geometry, there is a significant difference on the VTP area with the data from [42]. However, data obtained through the collaboration between Daher and ISAE-SUPAERO as part of the ISAAR research chair shows that the real value is around 3.00 m², which means the error is actually around 5%. The same holds for the HTP for which the use of data from Daher yields a difference of merely 1.5%. The computed difference between the wing area is negligible with the active constraint being the lift in low speed condition. This indicates that the amount of fuel consumed during the sizing mission is lesser than the Maximum Fuel Weight (MFW). It was computed to be around 870 kg which equals to a 2.8% difference with the reference value.

Table 7 – Main outputs for the Daher TBM 900 run.

Parameter	Output value	Reference value	Diff. (%)
MTOW (kg)	3358	3370	0.4
OWE (kg)	2114	2109	0.8
Fuel mission (kg)	763	774	1.4
Wing area (m ²)	18.07	18.0	0.4
HTP area (m ²)	4.94	4.76	3.78
VTP area (m ²)	2.85	2.56	11.3
Aircraft length (m)	10.736	10.736	0.0 ¹

4.3 Synthesis for reference aircraft

All in all, the results shows good agreement on both aircraft. It is worth noting that while some results might not be exact, data obtained thanks to FAST-OAD-GA were compared to aircraft which have been designed using much more precise tools. In addition to that, the average FAST-OAD-GA runs takes around 5-10 minutes, which means that a lot of design can be investigated to identify design trends before moving on to more precise analysis. Finally, thanks to some OpenMDAO features, it is also possible to interface FAST-OAD-GA with more advanced analysis tool for their results to be taken into account in early design stage.

5. Future development

As of now, FAST-OAD-GA provides models adequate for the sizing of general aviation aircraft which uses purely fuel-based propulsion. These however correspond to traditional architecture and propulsion chain. This prompted the start of an ongoing work which goal is to provide sizing methodologies that will enable the assessment of the performances of unconventional aircraft architectures and the study of a more to all electric powertrain.

5.1 Change in the mission module

In the former implementation of FAST-OAD-GA's performances module, the climb and descent phases were driven by a user-inputted thrust rate. Using a simplified version of the equilibrium equation in climb condition [15], the climb rate could be computed and the vertical speed was obtained based on the excess thrust available. The slipstream effects induced by distributed propulsion will however, as discussed in section 3.1, change the aerodynamics of the aircraft based on the propulsion performances which means that the point of equilibrium will change and can no longer be explicitly solved. Consequently, if the performances of the aircraft are to be computed and the benefits of distributed propulsion to be assessed, there is a need of modeling these effects with a level of detail adequate for preliminary aircraft design. Surrogate models such as the one presented in [44] [45] model those slipstream effects using deltas that are then added to the clean aerodynamic coefficients. These deltas are dependent on the clean coefficients and the thrust, which means that the thrust rate can no longer be set as an input to solve the full equilibrium. As discussed before, this also induces the need for an iterative loop on the aircraft flight parameters (AOA, thrust and δ_m) to achieve equilibrium because of the non-linearity of some models. For those reasons and to be able to fully use OpenMDAO capabilities, the performances module was rewritten. The computation of the equilibrium is

¹Aircraft length was used as an input for this run

now done using an Implicit Component whose residuals (which are to be driven to 0.0) are defined as the sum of forces and moments of the longitudinal equilibrium and whose outputs are the thrust, angle of attack and elevator angle. This then allows to compute the aerodynamic deltas in a separate component which is then fed back into the equilibrium computation, allowing for the iterative solving of the 3 equations - 3 unknowns system presented in equation 5. This also enables the integration of more thorough propulsion module such as the one described in Section 5.2 inside a separate component to emulate more realistic powertrains.

The fact that the propulsion and the computation of the slipstream effects are now in a separate component then allow each user, using the submodels feature implemented in FAST-OAD [14], to define its own model(s) for the computation of the impact of propulsion on the aerodynamics. This renders the computation of the equilibrium independent from the technology used for the propulsion which makes it possible to simulate the impact on the overall aircraft design of distributed propeller such as on NASA X57 or ducted fans such as on ONERA's Ampere concept plane [46]. One limitation has been identified so far. The solving of the 3 equations - 3 unknowns system returns the thrust at aircraft level while, for the computation of the slipstream, the thrust of each propulsion module is required. This means that a distribution of the thrust has to be imposed. For now, the thrust is assumed to be equally distributed on all propulsion module but some power architecture, like the one of NASA's X57, rely on having some engines producing more thrust than others depending on the flight phase.

This new module solves all the mission points simultaneously instead of one after the other as it was the case in the time step integration. Each equilibrium is thus represented as an element in the array containing the aircraft information such as the flight conditions and the masses at the different stages of the flight. An additional solver iterates on the mass array taking into account the potential weight variation due to fuel consumption, the changes in the thrust required to maintain equilibrium and the change in the center of gravity of the aircraft. This vectorial solving of the mission and the modularity described in earlier paragraph is illustrated in Figure 8.

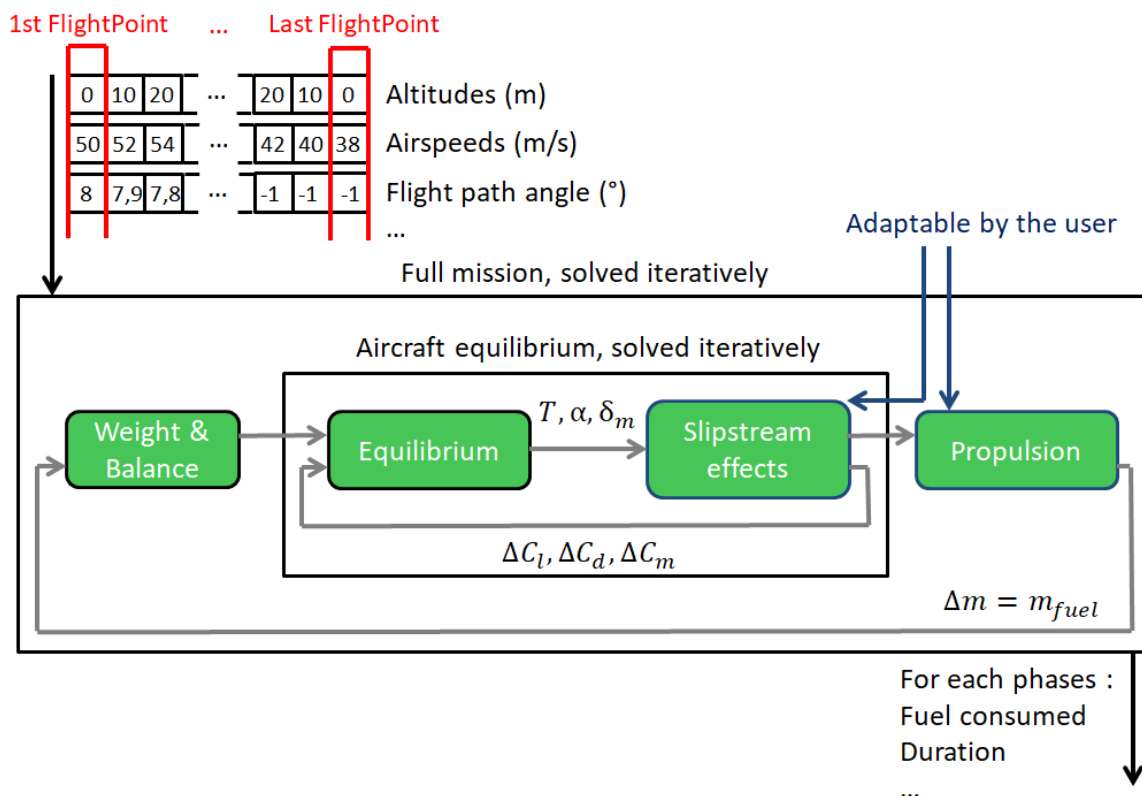


Figure 8 – Solving methodology and modularity of the new mission module

The final advantage of this rewriting of the mission modules is that, since the aircraft equilibrium is now defined as its own independent module, it can be called elsewhere in the code thanks to the sub-

model feature. This will then allow to assess the performances of the aircraft in low speed conditions while keeping the computation of the slipstream effects consistent with the other phases. This means it will now be possible to modify the sizing of the wing to take into account the effects of distributed propulsion and to quantify the gains at the overall aircraft level. The proposed implementation for this computation is the minimization of the wing area under the constraints that the equilibrium must be achievable with a feasible angle of attack, thrust and elevator command.

5.2 Change in the powertrain model

To allow FAST-OAD-GA to perform overall aircraft design of electric and hybrid-electric aircraft such as the concept plane presented in [47], existing models adapted to fuel-based propulsion will be extended to hybrid-electric solutions, and a methodology to accurately describe power architectures must be implemented. The latter allows an aircraft designer to account for certifiable fault-tolerant powertrains at a preliminary overall aircraft design stage. For those purposes, the load flow analysis method presented in [48] was chosen to be adapted for an implementation inside FAST-OAD-GA.

This methodology allows for the sizing and the computation of the performances of powertrain created based on its component library. It also allows for the assessment of the impact of component failures on the rest of the system as it automatically balance voltages and current level to have a converged electrical circuit. This means that tradeoff studies can be conducted between the oversizing of cables and buses to allow for load flow to be redirected and the addition of redundancies for the handling of component default. The integration of this methodology inside FAST-OAD-GA will also make it possible to study the impact of those failures at aircraft level, such as the verification of the climb performances or the reserve requirements, and what it implies on the oversizing of power sources and propulsive components.

The library of core components introduced in [48] is completed in a standalone version of the code with supplementary models to better describes the propulsive part of the systems and the power sources. The geometry and weight of the electric motor are computed using models from [49] while the electric performances are obtained following the methods described in [50]. For the battery sizing, the methodology from [51] is used so that the effect of C-rate and battery state of charge on current voltage are taken into consideration. Finally a fuel cell model that takes into account the cells polarization curves is integrated following the model described in [52]. All of those components are written in the OpenMDAO formalism so that they are compatible with the load flow analysis methodology and so that full use of the capabilities of the framework can be made.

6. Conclusion

This paper presents the first open-source release of FAST-OAD-GA, a set of aircraft sizing models tailored for general aviation. The objective of FAST-OAD-GA is to propose a MDAO tool which allows for the sizing of general aviation aircraft with innovative architecture and powertrains. FAST-OAD-GA is developed as an extension of the FAST-OAD framework, a MDAO platform for aircraft design. The need for sizing models for general aviation arose because the sizing models of commercial aviation of FAST-OAD were not adapted for CS-23 aircraft, partly because of the validity domain of the equations, of the differences on a technological level and the certification specifications. Thanks to the modularity brought by FAST-OAD and its plugin functionality, it was possible to create an alternative set of modules adapted for light aircraft. For this first release, specific models for CS-23 aircraft were developed, using either physics-based or empirical approaches. The work for the development of FAST-OAD-GA started with changes in the mass and geometry modules. The upcoming works focus on the mission and propulsion modules, in particular distributed propulsion, developed by a load flow method, allowing the user to see the influence of a change of architecture on the design aircraft overall.

7. Contact Author Email Address

mailto: Florent.LUTZ2@isae-superaero.fr

8. Supplementary materials

FAST-OAD is available online at <https://github.com/fast-aircraft-design/FAST-OAD>, FAST-OAD-GA is available online at <https://github.com/supaero-aircraft-design/FAST-GA>.

9. Copyright Statement

The authors confirm that they, and/or their company or organization, hold copyright on all of the original material included in this paper. The authors also confirm that they have obtained permission, from the copyright holder of any third party material included in this paper, to publish it as part of their paper. The authors confirm that they give permission, or have obtained permission from the copyright holder of this paper, for the publication and distribution of this paper as part of the ICAS proceedings or as individual off-prints from the proceedings.

10. Fundings

The presented work is supported by Daher through the research chair ISAAR “Innovative Solutions for Aviation Architecture & Regulation”.

References

- [1] Delbecq, S., Fontane, J., Gourdain, N., Mugnier, H., Planes, T., and Simatos, F., “Référentiel isae–supaero aviation et climat,” 2021.
- [2] Palladino, V., Jordan, A., Bartoli, N., Schmollgruber, P., Pommier-Budinger, V., and Benard, E., “Preliminary studies of a regional aircraft with hydrogen-based hybrid propulsion,” in *AIAA AVIATION 2021 FORUM*, p. 2411, 2021.
- [3] Yang, B., Lou, F., and Key, N. L., “Conceptual design of a 10-passenger thin-haul electric aircraft,” in *2020 AIAA/IEEE Electric Aircraft Technologies Symposium (EATS)*, pp. 1–18, IEEE, 2020.
- [4] Moore, K. R. and Ning, A., “Distributed electric propulsion effects on existing aircraft through multidisciplinary optimization,” in *2018 AIAA/ASCE/AHS/ASC Structures, Structural Dynamics, and Materials Conference*, p. 1652, 2018.
- [5] Ko, A., Schetz, J. A., and Mason, W. H., “Assessment of the potential advantages of distributed-propulsion for aircraft,” in *XVI International Symposium on Air Breathing Engines (ISABE)*, Citeseer, 2003.
- [6] MacDonald, T., Clarke, M., Botero, E. M., Vegh, J. M., and Alonso, J. J., *SUAVE: An Open-Source Environment Enabling Multi-Fidelity Vehicle Optimization*.
- [7] Drela, M., “Tasopt 2.00,” tech. rep., Tech. rep., Massachusetts Institute of Technology, 2010.
- [8] Gray, J. S., Hwang, J. T., Martins, J. R., Moore, K. T., and Naylor, B. A., “Openmdao: An open-source framework for multidisciplinary design, analysis, and optimization,” *Structural and Multidisciplinary Optimization*, vol. 59, no. 4, pp. 1075–1104, 2019.
- [9] David, C., Delbecq, S., Defoort, S., Schmollgruber, P., Benard, E., and Pommier-Budinger, V., “From fast to fast-oad: An open source framework for rapid overall aircraft design,” in *IOP Conference Series: Materials Science and Engineering*, vol. 1024, p. 012062, IOP Publishing, 2021.
- [10] Sgueglia, A., *Methodology for sizing and optimising a Blended Wing-Body with distributed electric ducted fans*. PhD thesis, ISAE-Institut Supérieur de l’Aéronautique et de l’Espace, 2019.
- [11] Raymer, D. P. and Design, A., “A conceptual approach,” *Design-A Seperate Discipline*, pp. 1–10, 1999.
- [12] Dupont, W. and Colongo, C., “Preliminary design of commercial transport aircraft,” *ISAESupaero, Toulouse, France*, 2012.
- [13] ROUX, É., *Modèles Moteur: Réacteurs double flux civils et réacteurs militaires à faible taux de dilution avec PC*. PhD thesis, Thèse: Pour une Approche Analytique de la Dynamique du Vol, 2002.
- [14] ONERA ISAE-SUPAERO, “FAST-OAD Documentation.” <https://fast-oad.readthedocs.io/en/latest>, 2021. Accessed: 2022-02-08.
- [15] Gudmundsson, S., *General aviation aircraft design: Applied Methods and Procedures*. Butterworth-Heinemann, 2013.
- [16] Roskam, J., *Airplane Design: Part 6-Preliminary Calculation of Aerodynamic, Thrust and Power Characteristics*. DARcorporation, 1985.
- [17] McDonald, R. A. and Gloudemans, J. R., “Open vehicle sketch pad: An open source parametric geometry and analysis tool for conceptual aircraft design,” in *AIAA SCITECH 2022 Forum*, p. 0004, 2022.
- [18] Torenbeek, E., “Synthesis of subsonic airplane design, 1982,” *Delft: Springer*.
- [19] Raymer, D. P., “Aircraft design: a conceptual approach (aiaa education series),” *Reston, Virginia*, 2012.

- [20] Al-Shamma, O., Ali, R., and Hasan, H. S., "An educational rudder sizing algorithm for utilization in aircraft design software," *International Journal of Applied Engineering Research*, vol. 13, no. 10, pp. 7889–7894, 2018.
- [21] EASA, *Certification Specifications and Acceptable Means of Compliance for Normal, Utility, Aerobatic, and Commuter Category Aeroplanes CS-23 Amendment 4, July 2015*.
- [22] Nicolai, L. M. and Carichner, G. E., *Fundamentals of aircraft and airship design, Volume 1—Aircraft Design*. American Institute of Aeronautics and Astronautics, 2010.
- [23] Wells, D. P., Horvath, B. L., and McCullers, L. A., "The flight optimization system weights estimation method," 2017.
- [24] Roskam, J., *Airplane Design: Part 5-Component Weight Estimation*. DARcorporation, 1985.
- [25] Habermann, A. L., "Effects of distributed propulsion on wing mass in aircraft conceptual design," in *AIAA AVIATION 2020 FORUM*, p. 2625, 2020.
- [26] Alonso Castilla, R., Lutz, F., Jézégou, J., and Bénard, E., "Wing structural model for overall aircraft design of distributed electric propulsion general aviation and regional aircraft," *Aerospace*, vol. 9, no. 1, p. 5, 2022.
- [27] Roux, E., "Modèle de masse voilure: Avions de transport civil," *Ph. D. Dissertation, SupAéro-ONERA, Toulouse, France*, 2006.
- [28] Hartman, E. P. and Biermann, D., "The aerodynamic characteristics of full-scale propellers having 2, 3, and 4 blades of clark y and raf 6 airfoil sections," 1938.
- [29] Biermann, D. and Hartman, E. P., *The aerodynamic characteristics of six full-scale propellers having different airfoil sections*. US Government Printing Office, 1939.
- [30] Verstraete, D. and MacNeill, R., "The effects of blockage on the performance of small propellers," in *20th Australasian Fluid Mechanics Conference*, 2016.
- [31] Veldhuis, L., "Review of propeller-wing aerodynamic interference," in *24th International Congress of the Aeronautical Sciences*, vol. 6, 2004.
- [32] Cirrus Design Corporation, "Pilot's Operating Handbook and FAA approved Airplane Flight Manual for the Cirrus SR22." <https://inflightpilottraining.com/wp-content/uploads/2018/12/SR22-POH.pdf>, 2016. Accessed: 2022-02-01.
- [33] Mattingly, J. D., *Elements of gas turbine propulsion*, vol. 1. McGraw-Hill New York, 1996.
- [34] DAHER-SOCATA, *Pilot Information Manual (PIM) of the Daher TBM 700*. Daher, 1988.
- [35] Hill, P. G. and Peterson, C. R., "Mechanics and thermodynamics of propulsion," *Reading*, 1992.
- [36] J.L. Montanés, *Actuaciones de Aerorreactores*. Universidad Politécnica de Madrid, 2019.
- [37] Cumpsty, N. and Heyes, A., *Jet propulsion*. Cambridge University Press, 2015.
- [38] Lutz, F., Reyssset, A., and Jezegou, J., "FAST-(OAD)-GA: Future Aircraft Sizing Tool - Overall Aircraft Design (General Aviation extension)," 7 2021.
- [39] Taylor, J. W. and others, *Jane's all the world's aircraft*. Jane's, 1981.
- [40] Beech Aircraft Corporation, "Pilot's Operating Handbook and FAA approved Airplane Flight Manual for the Beechcraft Duchess 76." <https://jasonblair.net/wp-content/uploads/2015/09/1978-BE76-Duchess-POH.pdf>, 1978. Accessed: 2022-05-06.
- [41] DAHER-SOCATA, *Pilot Information Manual (PIM) of the Daher TBM 900*. Daher, 2013.
- [42] Gunston, B., "Jane's all the world's aircraft: development and production: 2015-16," *IHS Global*, vol. 1221, 2015.
- [43] DAHER-SOCATA, "TBM 900 Comprehensive Guide." https://o.b5z.net/i/u/10113707/f/TBM_900_-_Comprehensive_Guide.pdf, 2014. Accessed: 2022-05-10.
- [44] Patterson, M. D., *Conceptual design of high-lift propeller systems for small electric aircraft*. PhD thesis, Georgia Institute of Technology, 2016.
- [45] de Vries, R., Brown, M. T., and Vos, R., "A preliminary sizing method for hybrid-electric aircraft including aero-propulsive interaction effects," in *2018 Aviation Technology, Integration, and Operations Conference*, p. 4228, 2018.
- [46] Dillinger, E., Döll, C., Liaboeuf, R., Toussaint, C., Hermetz, J., Verbeke, C., and Ridet, M., "Handling qualities of onera's small business concept plane with distributed electric propulsion," in *31st Congress of the International Council of the Aeronautical Sciences*, 2018.
- [47] Hermetz, J., Ridet, M., and Doll, C., "Distributed electric propulsion for small business aircraft a concept-plane for key-technologies investigations," in *ICAS 2016*, 2016.
- [48] Hendricks, E. S., Chapman, J., and Aretskin-Hariton, E., "Load flow analysis with analytic derivatives for electric aircraft design optimization," in *AIAA Scitech 2019 Forum*, p. 1220, 2019.

- [49] Thauvin, J., *Exploring the design space for a hybrid-electric regional aircraft with multidisciplinary design optimisation methods*. PhD thesis, 2018.
- [50] McDonald, R. A., "Electric propulsion modeling for conceptual aircraft design," in *52nd Aerospace Sciences Meeting*, p. 0536, 2014.
- [51] Vratny, P. C., Gologan, C., Pornet, C., Isikveren, A. T., and Hornung, M., "Battery pack modeling methods for universally-electric aircraft," in *4th CEAS Air & Space Conference*, pp. 525–535, Linköping University Electronic Press Linköping, Sweden, 2013.
- [52] Hoogendoorn, J., "Fuel cell and battery hybrid system optimization: Towards increased range and endurance," 2018.